A multiple myeloma classification system that associates normal B-cell subset phenotypes with prognosis

Julie Støve Bødker,[1,*] Rasmus Froberg Brøndum,[1,*] Alexander Schmitz,[1,*] Anna Amanda Schönherz,[2] Ditte Starberg Jespersen,[1] Mads Sønderkær,[1] Charles Vesteghem,[2] Hanne Due,[1] Caroline Holm Nørgaard,[1] Martin Perez-Andres,[1,3] Mehmet Kemal Samur,[4] Faith Davies,[5] Brian Walker,[5] Charlotte Pawlyn,[6] Martin Kaiser,[6] David Johnson,[6] Uta Bertsch,[7] Annemiek Broyl,[8] Mark van Duin,[8] Rajen Shah,[9] Preben Johansen,[10] Martin Agge Nørgaard,[11] Richard J. Samworth,[9] Pieter Sonneveld,[8] Hartmut Goldschmidt,[7] Gareth J. Morgan,[5] Alberto Orfao,[3] Nikhil Munshi,[4] Hans Erik Johnsen,[1,2,12] Tarec El-Galaly,[1,2,12] Karen Dybkær,[1,2,12,†] and Martin Bøgsted[1,2,12,†]

[1]Department of Haematology, Aalborg University Hospital, Aalborg, Denmark; [2]Department of Clinical Medicine, Aalborg University, Denmark; [3]Institute of Biomedical Research of Salamanca, University of Salamanca, Salamanca, Spain; [4]Dana-Farber Cancer Institute, Harvard Medical School, Boston, MA; [5]UAMS Myeloma Institute, University of Arkansas for Medical Sciences, Little Rock, AR; [6]Division of Molecular Pathology, Institute of Cancer Research, London, United Kingdom; [7]National Center for Tumor Diseases, University of Heidelberg, Heidelberg, Germany; [8]Department of Haematology, Erasmus Medical Center, Rotterdam, The Netherlands; [9]Centre for Mathematical Sciences, University of Cambridge, Cambridge, United Kingdom; and [10]Department of Haematopathology, [11]Department of Cardiothoracic Surgery, and [12]Clinical Cancer Research Center, Aalborg University Hospital, Aalborg, Denmark

Key Points

- We have identified hierarchal subtype differences in myeloma cells at diagnosis.

- The prognostic impact supports an acquired B-cell trait and phenotypic plasticity as a pathogenetic hallmark of MM.

Despite the recent progress in treatment of multiple myeloma (MM), it is still an incurable malignant disease, and we are therefore in need of new risk stratification tools that can help us to understand the disease and optimize therapy. Here we propose a new subtyping of myeloma plasma cells (PCs) from diagnostic samples, assigned by normal B-cell subset associated gene signatures (BAGS). For this purpose, we combined fluorescence-activated cell sorting and gene expression profiles from normal bone marrow (BM) Pre-BI, Pre-BII, immature, naïve, memory, and PC subsets to generate BAGS for assignment of normal BM subtypes in diagnostic samples. The impact of the subtypes was analyzed in 8 available data sets from 1772 patients' myeloma PC samples. The resulting tumor assignments in available clinical data sets exhibited similar BAGS subtype frequencies in 4 cohorts from de novo MM patients across 1296 individual cases. The BAGS subtypes were significantly associated with progression-free and overall survival in a meta-analysis of 916 patients from 3 prospective clinical trials. The major impact was observed within the Pre-BII and memory subtypes, which had a significantly inferior prognosis compared with other subtypes. A multiple Cox proportional hazard analysis documented that BAGS subtypes added significant, independent prognostic information to the translocations and cyclin D classification. BAGS subtype analysis of patient cases identified transcriptional differences, including a number of differentially spliced genes. We identified subtype differences in myeloma at diagnosis, with prognostic impact and predictive potential, supporting an acquired B-cell trait and phenotypic plasticity as a pathogenetic hallmark of MM.

Introduction

Despite the extensive insight into multiple myeloma (MM) pathogenesis, as outlined in the World Health Organization classification,[1,2] a number of questions remain unanswered regarding the origin and initiation of the developing myeloma cells, including its association with the normal B-cell hierarchy in

the bone marrow (BM).[3-6] We hypothesize that considering MM as a disease of differentiation by identifying its cell of origin (COO) could lead to novel biological insight and development of new treatment options as described by Boise et al.[7]

MM develops from a premalignant monoclonal gammopathy of unknown significance (MGUS), by a stepwise oncogenesis to intramedullary early smoldering or evolving de novo myeloma because of acquired genetic deregulation.[8-10] The primary translocations implicating the 14q32 locus involve a series of promiscuous target genes, with *CCND1* and *FGFR3/MMSET* being the most frequently present at the MGUS stage.[11] Furthermore, the larger part of break points occurs in the switch regions, suggesting the early translocation happens during immunoglobulin heavy chain class-switch recombination in the germinal center.[12-14] The existence of early translocations and the overexpression of *CCND* genes form the translocations and cyclin D (TC) classification generated from early events.[9,11] Later incidences include a spectrum of mutations and dysregulations occurring in advanced disease with poor prognosis.[14-19]

Myeloma plasma cells (PCs) are class switched, freezing the initiating cell at the postgerminal B-cell maturation stage, refuting that the disease is initiated in earlier B-cell subsets, as has been proposed before.[20] The earliest immunoglobulin heavy chain clonotypic cell we have identified with a class-switched isotype is in the myeloma memory B-cell compartment,[21,22] but its clonogenic and malignant potential is a controversial issue.[23-26] Recent studies have concluded that the clonotypic cells are remnants of a neoplastic cell with no malignant potential,[27,28] contrasting the myeloma PC compartments.

The myeloma stem cell concept has been reviewed in detail by us and others.[29,30] We proposed an operational definition of COO to allow for acquisition of data supporting that a normal B cell, which achieves the first myeloma initiating mutation, is not necessarily linearly connected to the myeloma stem cell. These results underpin the hypothesis that myeloma generating cells are present in the malignant PC compartment, but the COO is a normal counterpart of a germinal-center B cell that evolves via differentiation into a premalignant PC compartment already present in MGUS populations.

The plasticity potential of myeloma cells, perhaps caused by interaction with the tumor microenvironment, also plays an important role in development and maintenance of MM.[30]

The present study takes a COO approach, where we refer to an expanding compartment initiated by a differentiation specific oncogene hit.[31] The terms "COO" and "cancer stem cells" have been used interchangeably. However, it is important to differentiate between them as in contrast to our phenotypic COO studies, it is our perception that cancer stem cell research depends on single cell studies in the frame of the classical stem cell definition.[29]

The deregulated B-cell cells under influence by the microenvironment may be key in the emergence of myeloma and its related phenotypic changes. This phenomenon, coined "plasticity," is defined as a changed cellular phenotype or function during deregulated differentiation.[32] More specifically, this refers to malignant mature PCs that share properties of different maturation steps, including precursors. The phenomenon facilitates a new tool for providing insight into the observed clonal plasticity[33,34] associated with oncogenesis.[8-12,17,35-38] The mechanisms of deregulated differentiation and myeloma-cell plasticity ought to be investigated and their clinical significance assessed.

Recently, we have documented a procedure to identify and study gene expression of flow-sorted human B-cell subsets from normal lymphoid tissue.[39-42] These subsets can be profiled and by proper statistical modeling defined specific B-cell associated gene signatures (BAGS), recently introduced for diffuse large B-cell lymphoma (DLBCL).[43-45] Here we have applied BAGS from normal BM subsets to assign individual MM subtypes and correlate them with prognosis to delineate their pathogenetic impact.

Patients, material, and methods

The subtyping method based on normal BM has previously been briefly outlined in Nørgaard et al[46] and applied to chronic lymphocytic leukemia patients. In this article, we will describe it in more detail and provide more profound quality control of the normal samples.

Ethical statement and tissue collection

All normal tissue samples were collected in accordance with the research protocol (Myeloma Stem Cell Network, N-20080062MCH) accepted by the North Denmark Regional Committee on Health Research Ethics.

Normal BM was either harvested from the sternum (n = 7)[41] during cardiac surgery or taken as aspirates from the iliac crest of healthy volunteers (n = 14) during routine surgical procedures in accordance with the Declaration of Helsinki. Normal BM aspirates were cleared for red blood cells by 15 minutes lysis using 20-fold excess of Easylyse (DAKO, Glostrup, Denmark). The sample was centrifuged 10 minutes at 250*g*, the supernatant discarded, and the pellet washed in phosphate-buffered saline. The centrifugation step was repeated, and the pelleted cells dissolved in stain buffer and processed directly for analysis using multiparametric flow cytometry (MFC).

MFC, cell sorting, and gene expression profiling

The normal B-cell subsets were phenotyped by MFC and fluorescence-activated cell sorting (FACS) into 6 distinct B-cell subsets (Pre-BI, Pre-BII, immature [Im], naïve [N], memory [M] B cells, and PCs) using a monoclonal antibody panel,[41,44] described in detail in supplemental Text 1.

RNA was labeled for microarray analysis, hybridized to the Affymetrix Human Exon 1.0 ST (HuEx-1.0-st) Array[41,44] or to the Affymetrix Human Genome U133 Plus 2.0 (HU-U133-2.0) Array platform, and referred to as the "normal sternal BM data set" (n = 7) (GSE68878),[47] the "normal iliac crest BM aspirate" data set–HuEx-1.0-st (n = 8) (GSE99635), and the "normal iliac crest BM aspirate" data set–Hu-U133-2.0 (n = 6) (GSE107843). The CEL files have been deposited in the National Center for Biotechnology Information Gene Expression Omnibus repository with GSE numbers as indicated previously and comply with minimum information about a microarray experiment (MIAME) requirements.[48]

Clinical myeloma data sets

Clinical data originated from Affymetrix microarray analysis of PC-enriched myeloma samples, from 4 prospective clinical trials: University of Arkansas for Medical Sciences (UAMS), Hematology Oncology Group-65/German-speaking Myeloma Multicenter Group-HD4, Medical Research Council Myeloma IX
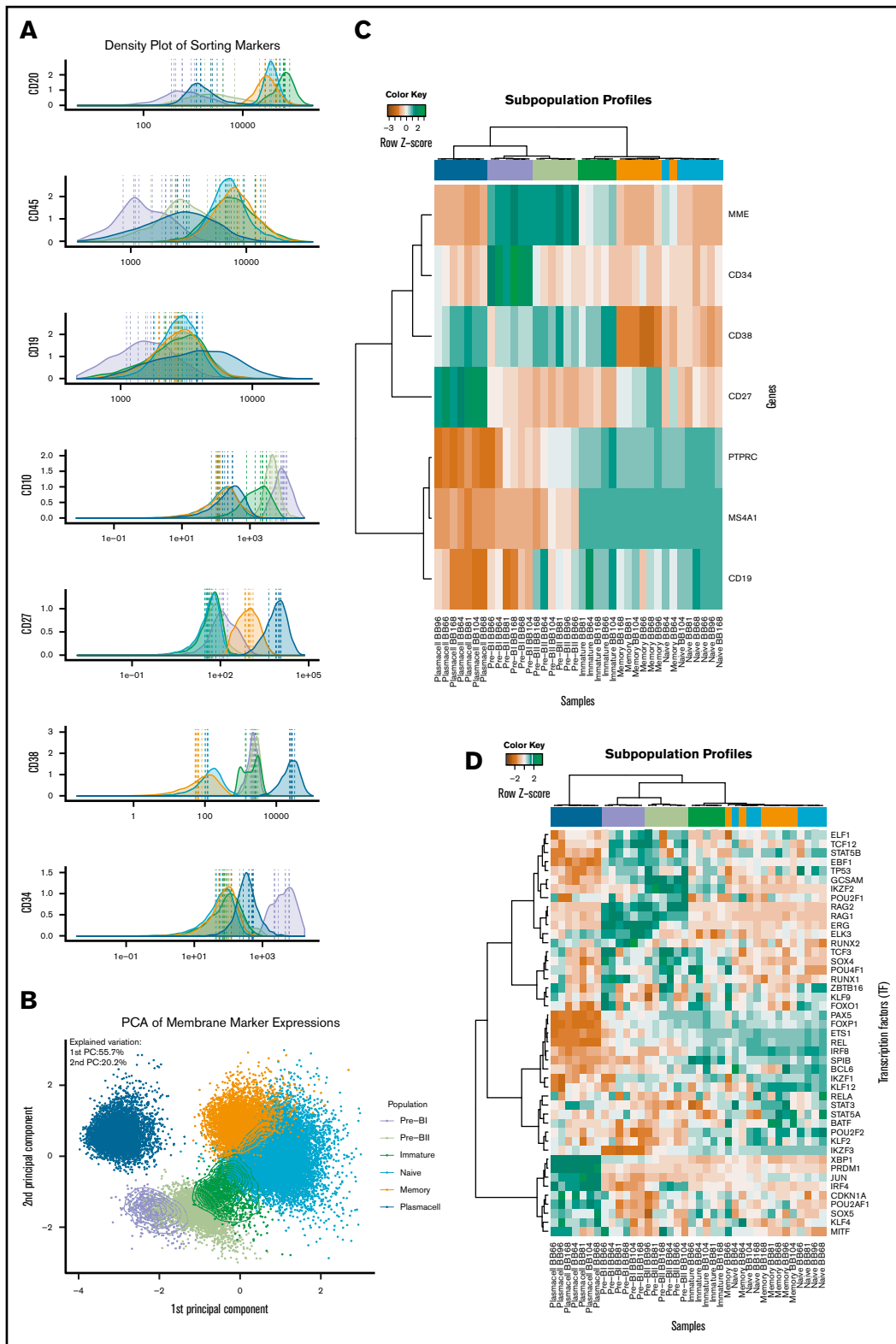
Figure 1. Expression of membrane markers, transcription factors, and B-cell subset-specific genes in normal BM tissue. (A) B cells of the BM were defined by flow cytometry as CD19^{+}, CD45^{+}, and CD3^{−} and were additionally divided by surface marker expression of CD10, CD20, CD27, CD38, and CD34, published in detail previously.[44] The data quality of the differentiating B-cell subset compartments was validated as illustrated by normalized histograms of (A) the mean fluorescence intensities (MFIs) CD markers based on merged MFC reanalysis of pure sorted populations resulting from 7 independent sorting procedures. Broken lines represent MFI values for each sorted B-cell subset. (B) Principal component analysis of the MFI values for each sorted cell in all samples. The cells are coded with a color according to their original subset.

(All HG-U133-2.0 arrays), and Acute Medically Ill Venous Thrombo-embolism Prevention with Extended Duration Betrixaban (APEX) (Affymetrix Human Genome U133A [HG-U133A] arrays),[35,36,49-52] as well as a preclinical study, the Intergroupe Francophone du Myelome and Dana-Farber Cancer Institute Project[37,53] (HuEx-1.0-st arrays).

The following 3 cohorts were used for BAGS assignment and subtype association in the disease stages MGUS, smoldering multiple myeloma, relapsed multiple myeloma, primary plasma cell leukemia, and human myeloma cell lines: the Salamanca cohort (Affymetrix Human Gene 1.0 ST arrays),[54] the Milan cohort (HG-U133A arrays),[55] and the Mayo cohort (HG-U133A arrays).[56,57]

The following 2 B-cell line data sets were used in the analysis: Bcell20 (HuEx-1.0-st arrays) and Bcell26 (HG-U133-2.0 arrays).[58]

All data sets are retrieved from Gene Expression Omnibus with the indicated GSE numbers and are described in detail in the "Materials and methods" of supplemental Text 1.

Statistical analysis

All statistical analyses were performed with R version 3.4.3 using Bioconductor packages.[59,60] Detailed session information is provided as a Knitr document[61] in supplemental Text 2.

Array normalization. All gene expression data sets where cohort-wise background corrected, normalized, and summarized by robust multichip average (RMA)[62] normalization using the functions from the R-package affy v1.54.0[63] and summarized at Ensemble Gene ID level with a custom CDF file from brainarray version 20.0.0. The analyses are based on the online gene expression profile (GEP) data sets listed previously and summarized in supplemental Text 1.

Systematic evaluation of transcription factors, surface markers, and B-cell differentiation genes. Transcription factors, surface markers, and B-cell differentiation genes as defined in Biomart (http://www.biomart.org/) were listed and included in hierarchical clustering of the BM data set. The most variable and distinctive genes across subsets were selected and combined with B-cell subset specific genes identified through literature review to evaluate subset identity.

Multivariate statistical methods. Comparisons between GEPs of molecular subsets were performed by principal component analysis and heat maps. For this we used the prcomp and heatmap.2 functions from the R-packages stats and gplots, respectively. The hierarchical clusters alongside the heat maps were made using Ward's method with Pearson's correlation coefficient as dissimilarity measure via the R-function *hclust*.

TC and risk classification. Methods for deriving the TC expression pattern and the UAMS risk classification based on Affymetrix gene expression microarray data are described in Bergsagel et al and Zhan et al.[9,35]

BAGS classification. The BAGS classifier was trained on median centered gene expression data from normal BM, using a regularized multinomial regression model with 6 classes corresponding to the respective B-cell subtypes. Regularization was done using the elastic net penalty as implemented in the R-package glmnet.[64] The elastic net penalty depends on a model parameter α varying between 0 and 1, which balances the ridge regression penalty ($\alpha = 0$), allowing all genes in the model, and the Lasso penalty ($\alpha = 1$), allowing a maximum number of genes equal to the number of samples. The model also involves a regularization parameter λ that determines the weight of the penalty and thereby the number of nonzero coefficients. The model parameter α was varied between 0.01 and 1, and the regularization parameter λ was varied between -7.5 and -1 on a log scale. The adequacies of the models were validated by choosing the minimum multinomial deviance determined by "leave 1 sample out" cross validation. The model with $\alpha = 0.24$ and log $\lambda = -5.67$ had the smallest cross-validated multinomial deviance leaving us with 184 genes with nonzero coefficients (supplemental Figure 1). This indicates, that by lowering log λ below -5.67, a number of alternative very gene rich models could have described the data well. However, we found the above-mentioned choice a suitable compromise between sparsity and robustness. Each clinical data set was gene-set-wise adjusted to have zero median and same variance as the normal BM data set. The associated COO Pre-BI, Pre-BII, Im, N, M, or PC for each patient in each data set was subtyped by the BAGS classifier by assigning the class with the highest predicted probability score above 0.40 and otherwise unclassified (supplemental Figure 2).

The probability cutoff was thoroughly tested (supplemental Text 2, section 11.1).

REGS classification. The samples were assigned resistance probabilities for the drug melphalan by resistance gene signature (REGS) classifiers.[58,65-68]

Survival analysis. Kaplan-Meier curves, log-rank tests, and Cox proportional hazards models were used for survival analysis and handled with the R-package survival.[69] The cohorts involving patients from 3 prospective clinical trials were amalgamated into a meta–data set to increase the power of the study. BAGS subtypes as an independent explanatory variable was investigated in the meta–data set by a Cox proportional hazards regression analysis with BAGS subtypes, TC classes, and cohort as potential confounders. Harell's C-statistic for overall survival (OS) was calculated from predicted values from the multivariate Cox model with and without inclusion of the BAGS classes to assess the prognostic utility.

Detection of alternative splice variants in BAGS subclasses. Alternative splice variants in the BAGS subtypes were investigated using the analysis of splice variation (ANOSVA) method.[70] The method consists of a linear model with interaction effects to detect

Figure 1. (continued) The dots represent mean values for each sorted B-cell subset. (C) The most variable probe sets were used in unsupervised hierarchical clustering analysis of the surface markers (MME = CD10, CD34, CD38, CD27; PTPRC = CD45; MS4A = CD20, CD19) used for FACS. (D) B-cell differentiation–specific genes (n = 45), summarized from a literature review of transcriptional regulation of B lymphopoiesis. The colors at the top of panel D indicate the relative gene expression for each sample, with blue representing high and brown representing low.

Table 1. BAGS defined subtype analysis

Group	Pre-BI (%)	Pre-BII (%)	Im (%)	N (%)	M (%)	PC (%)	UC (%)	Sum
Frequencies across data sets (P = .90)								
UAMS	3 (1)	29 (5)	58 (10)	143 (26)	219 (39)	23 (4)	84 (15)	559
Hovon 65	2 (1)	19 (6)	45 (14)	61 (19)	134 (42)	11	48 (15)	320
Myeloma IX	1 (0)	14 (6)	23 (9)	59 (24)	105 (43)	8 (3)	37 (15)	247
IFM-DFCI	2 (1)	11 (6)	21 (12)	38 (22)	68 (40)	4 (2)	26 (15)	170
Sum*	8 (1)	75 (6)	147 (11)	302 (23)	528 (41)	46 (4)	196 (15)	1296
Association with the TC classification (P < .001)								
4p16	1 (1)	21 (12)	7 (4)	45 (25)	78 (44)	3 (2)	22 (12)	177
MAF	2 (2)	4 (5)	12 (15)	25 (30)	31 (38)	1 (1)	7 (9)	82
6p21	1 (1)	2 (2)	12 (14)	19 (22)	36 (42)	2 (2)	14 (16)	86
11q13	0 (0)	3 (2)	11 (7)	46 (29)	81 (51)	4 (2)	15 (9)	160
D1	2 (0)	11 (3)	63 (15)	89 (21)	157 (37)	19 (5)	81 (19)	422
D1plusD2	0 (0)	4 (20)	2 (10)	2 (10)	9 (45)	0 (0)	3 (15)	20
D2	1 (1)	16 (13)	12 (10)	15 (12)	53 (44)	7 (6)	17 (14)	121
Unclassified	1 (0)	12 (5)	28 (12)	60 (26)	81 (36)	10 (4)	36 (16)	228
Sum	8 (1)	73 (6)	147 (11)	301 (23)	526 (41)	46 (4)	195 (15)	1296
ISS stage III with increased frequencies in the Pre-BII and M subtypes (P = .032)								
Stage I	2 (0)	8 (2)	51 (12)	115 (28)	149 (36)	18 (4)	72 (17)	415
Stage II	1 (0)	18 (7)	25 (9)	65 (24)	105 (39)	15 (6)	39 (15)	268
Stage III	2 (1)	19 (10)	22 (11)	33 (17)	89 (46)	5 (3)	23 (12)	193
NA	1 (0)	17 (7)	28 (11)	50 (20)	115 (46)	4 (2)	35 (14)	250
Sum	6 (1)	62 (6)	126 (11)	263 (23)	458 (41)	42 (4)	169 (15)	1126

The BAGS-defined subtype analysis was performed across 4 different clinical cohorts (N = 1296 cases) following assignment of the data sets according to the restricted multinomial classifier.

ISS, International Staging System; UC, unclassified.

alternative exon usage between 1 class and the rest within a gene. The linear model is given by: $y_{ijk} = \mu + \alpha_i + \beta_j + \gamma_{ij} + \varepsilon_{ijk}$, where y_{ijk} is the $\log_2$ RMA normalized gene expression for class i, exon j, and sample k; μ is the mean expression for the gene; α_i is the class effect; β_j is the exon effect; γ_{ij} is the interaction between group i and exon j (ie, the alternative exon usage); and the ε_{ijk}'s are independent, identically distributed Gaussian residuals. The analysis was performed genewise for all genes of interest, and the result for each gene was reported as the effect size and P value for the most significant interaction effect. When fitting a linear model in R, the interaction effects are by default given as treatment effects (ie, 1 level is set as a reference with an effect of zero and other effects are estimated as deviations from this). This makes the estimation dependent on the choice of reference. As we are interested in deviations from the group effect, an internal loop over exons was initially run for each gene, where the expressions were groupwise median centered and the reference exon was chosen as the exon giving the highest P value in a 2-sided Student t test of the group means (ie, the exon where the difference between groups was closest to the median difference). For the analysis of differential exon usage, the uncentered data were used.

Data for the analysis were obtained by RMA normalizing the 170 samples with HuEx-1.0-st array data from the IFM-DFCI data set using the just.rma function from the R-package affy v1.54.0[63] and summarizing at exon level with a custom CDF file from brainarray version 20.0.0. All genes included in the training set for the BAGS classifier were investigated for differential exon usage for Pre-BII vs rest, and memory vs rest. Genes with evidence of differential exon usage were defined as genes with an adjusted $P < .01$ and an absolute interaction effect >1. Significant genes for the analysis of memory subtype cases vs rest are shown in supplemental Table 1B, and significant genes for the analysis of Pre-BII vs rest are shown in supplemental Table 2A.

An enrichment analysis for biological process gene ontology (GO) terms of significant genes was done using the R-package topGO v2.28.0. Results for memory vs rest are shown in supplemental Table 3B, and results for Pre-BII vs rest are shown in supplemental Table 3A. Updates in the GO.db database might cause changes in the enrichment analysis; accordingly, all tables and interpretations of GO terms in this document are at version 3.4.1 of the GO.db.[71]

The significance level was set throughout to 0.05, and effect estimates were provided with 95% confidence intervals. P values for the differential gene expression and alternative splice analyses were adjusted by Holm's method.[72]

Results

BAGS classifier generation and clinical sample assignment

The data quality of the differentiating B-cell subset compartments of the sternal BM was individually validated as illustrated by density
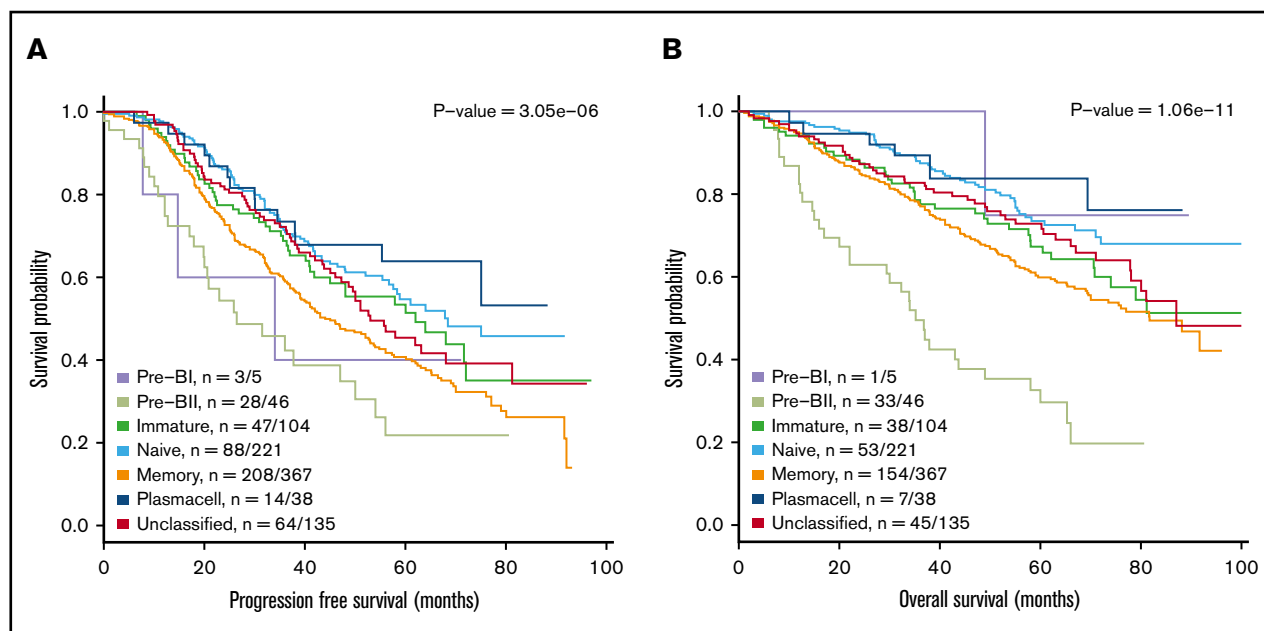
Figure 2. Meta-analysis of the prognostic impact of assigned BAGS subtypes. Progression-free survival (PFS) (A) and OS (B) were compared between BAGS subtypes for high-dose melphalan–treated patients in published prospective clinical trials. *P* values are results from log-rank tests. The subtype numbers given as n are the numbers of events/number of assigned patients with the subtypes in the meta–data set. The BAGS subtypes are color coded as in Figure 1.

plots from MFC analysis (Figure 1A) and principal component analysis (Figure 1B) of the MFIs of the CD markers used for FACS; unsupervised cluster analysis was also conducted for the gene expression values of the membrane CD markers used for FACS (Figure 1C; previously shown in Nørgaard et al[46]) and 45 classical B-cell markers summarized from a literature search (Figure 1D). Subset-specific segregation was further documented by principal component analysis (supplemental Figure 3).

The BAGS classifiers with the smallest deviance determined by cross validation consisted of 184 genes (for details, see supplemental Text 1 and supplemental Figure 1). Each B-cell subset signature contained 27 to 54 genes, ensuring comparable gene representation for all subsets in the BAGS classifier. The selected genes and associated coefficients for the BAGS signatures are shown in supplemental Table 4 (previously shown in Nørgaard et al[46]). The expressed signatures included 51 genes associated with specific B-cell functions, 79 specific genes with more fundamental biological associations, and 24 probes with unknown gene functions (supplemental Table 5A-F).

We subsequently validated the BAGS classifier, which was trained using GEP data from Human Exon 1.0 ST Arrays, on independent normal B-cell subsets from BM aspirates from the iliac crest profiled using either HuEx-1.0-st or HG-U133-2.0 arrays, and found concordant assignments for both platforms (supplemental Table 2). This documented the cross-platform validity of the classifier, allowing its use in clinical data with GEP originating from other platforms.

Microarray data from 4 independent cohorts (n = 1296) of de novo MM patients were assigned for BAGS subtypes. Table 1 shows the resulting assignment of the tumors and exhibited

BAGS subtype frequencies and average percentage for Pre-BI = 1%, Pre-BII = 6%, Im = 11%, N = 23%, M = 41%, and PC = 4%, with no significant variation between the cohorts from different geographic regions, time periods, or sampling methods (*P* = .9). We allow 15% of cases within each cohort to be unclassified, resulting in a probability cutoff of ~0.40. The distribution of the TC classes within the BAGS subtypes is given in Table 1, with significant association identified (*P* < .001). There was also significant correlation with ISS staging (*P* = .032), with increased numbers of the Pre-BII and M subtypes associated with ISS stage III, as shown in Table 1. BAGS, proliferation index, and melphalan resistance assignments for all samples used in the analyses are provided in supplemental Table 6A-H.

Prognostic impact of assigned BAGS subtypes

Figure 2 illustrates the results from a meta-analysis of the 916 patients included in the 3 prospective trial cohorts with high-dose melphalan as first-line therapy (UAMS, HOVON65/GMMG-HD4, and MRC Myeloma IX) with the HG-U133-2.0 microarray data available, documenting that the assigned BAGS subtypes were significantly associated with PFS and OS (PFS, log-rank test, *P* < .001; OS, log-rank test, *P* < .001). Major impact was observed within patient cohorts with the Pre-BII and M subtypes, which had a significantly inferior prognosis compared with the patients with Im, N, and PC subtypes.

The robustness of the BAGS association with outcome was successfully evaluated for a wide range of probability cutoffs for the percentage of unclassified cases (supplemental Text 2, section 11.1). The BAGS-assigned MM subtypes in the individual prospective clinical trial data sets UAMS/TT2&3, HOVON/GMMG-HD4, and MRCIX, all including high-dose melphalan and a variety of new drugs, were also separately analyzed for outcome following

Table 2. Cox proportional hazards regression analysis

	Univariate			Multivariate		
	Hazard ratio	95% CI	*P*	Hazard ratio	95% CI	*P*
Combined PFS, n = 642, number of events = 311						
Pre-BII	1	—	—	1	—	—
Im	0.45	0.26-0.76	.0032	0.48	0.28-0.83	00085
N	0.41	0.25-0.66	<.001	0.39	0.24-0.63	<.001
M	0.61	0.39-0.95	.027	0.58	0.37-0.92	.02
PC	0.28	0.13-0.6	<.001	0.3	0.14-0.64	.0018
4p16	1	—	—	1	—	—
MAF	0.47	0.29-0.77	.0026	0.53	0.32-0.86	.011
6p21	0.23	0.07-0.73	.013	0.17	0.05-0.54	.0027
11q13	0.36	0.26-0.52	<.001	0.31	0.22-0.45	<.001
D1	0.35	0.26-0.47	<.001	0.3	0.22-0.41	<.001
D1plusD2	0.27	0.12-0.63	.0024	0.27	0.12-0.62	.0021
D2	0.38	0.25-0.57	<.001	0.25	0.16-0.39	<.001
Hovon65	1	—	—	1	—	—
MyelomaIX	1.16	0.84-1.6	.38	1.15	0.83-1.59	.41
UAMS	0.37	0.29-0.48	<.001	0.33	0.26-0.42	<.001
Combined OS, n = 642, number of events = 236						
Pre-BII	1	—	—	1	—	—
Im	0.31	0.18-0.51	<.001	0.36	0.21-0.62	<.001
N	0.19	0.12-0.3	<.001	0.19	0.12-0.31	<.001
M	0.33	0.22-0.5	<.001	0.34	0.23-0.52	<.001
PC	0.1	0.03-0.28	<.001	0.11	0.04-0.32	<.001
4p16	1	—	—	1	—	—
MAF	0.53	0.3-0.93	.027	0.59	0.34-1.05	.072
6p21	0.43	0.13-1.36	.15	0.51	0.16-1.65	.26
11q13	0.48	0.33-0.71	<.001	0.51	0.35-0.76	<.001
D1	0.37	0.26-0.51	<.001	0.39	0.28-0.55	<.001
D1plusD2	0.41	0.17-1.02	.056	0.31	0.12-0.78	.013
D2	0.53	0.34-0.83	.0056	0.47	0.3-0.75	.0014
Hovon65	1	—	—	1	—	—
MyelomaIX	1.23	0.81-1.85	.33	1.24	0.82-1.88	.31
UAMS	0.91	0.68-1.21	.5	0.87	0.65-1.17	.35

Cox proportional hazards regression analysis in the meta–data set for BAGS subtypes based on PFS and OS, demonstrating added independent significance to the TC classification staging system. Columns on the left show results for a univariate analysis with each of the covariates, whereas columns on the right show results from the multivariate model. The Pre-BI class was dropped from the analysis because of too few observations in this group.

CI, confidence interval.

treatment as illustrated in supplemental Figure 4. Results from the individual data sets were in accordance with the above-described meta-analysis illustrated in Figure 2.

Cox proportional hazard meta-analysis results, as shown in Table 2, and Harell's C-statistic, giving the concordance between observed survival and predicted risk scores from the a multivariate cox model with (C = 0.65) and without (C = 0.59) BAGS classes, demonstrated that the BAGS subtypes added significant and independent prognostic information to the already well-established TC classification. In addition, we found significant correlation between the BAGS subtypes and the proliferation index (PI) risk

profiling (*P* < .001), melphalan resistance probability (*P* < .001), and β-2 microglobulin plasma level (*P* < .001) as illustrated in Figure 3, respectively. Results in these figures are for a combined data set adjusted for differences in individual data sets, while results for individual data sets may be found in supplemental Text 1 and supplemental Figure 5.

BAGS assignment of MGUS, smoldering myeloma, MM, extramedullary MM, and myeloma cell lines

Available data sets were used for BAGS assignment of associated myeloma diseases, as shown in supplemental Table 7A. Of interest,
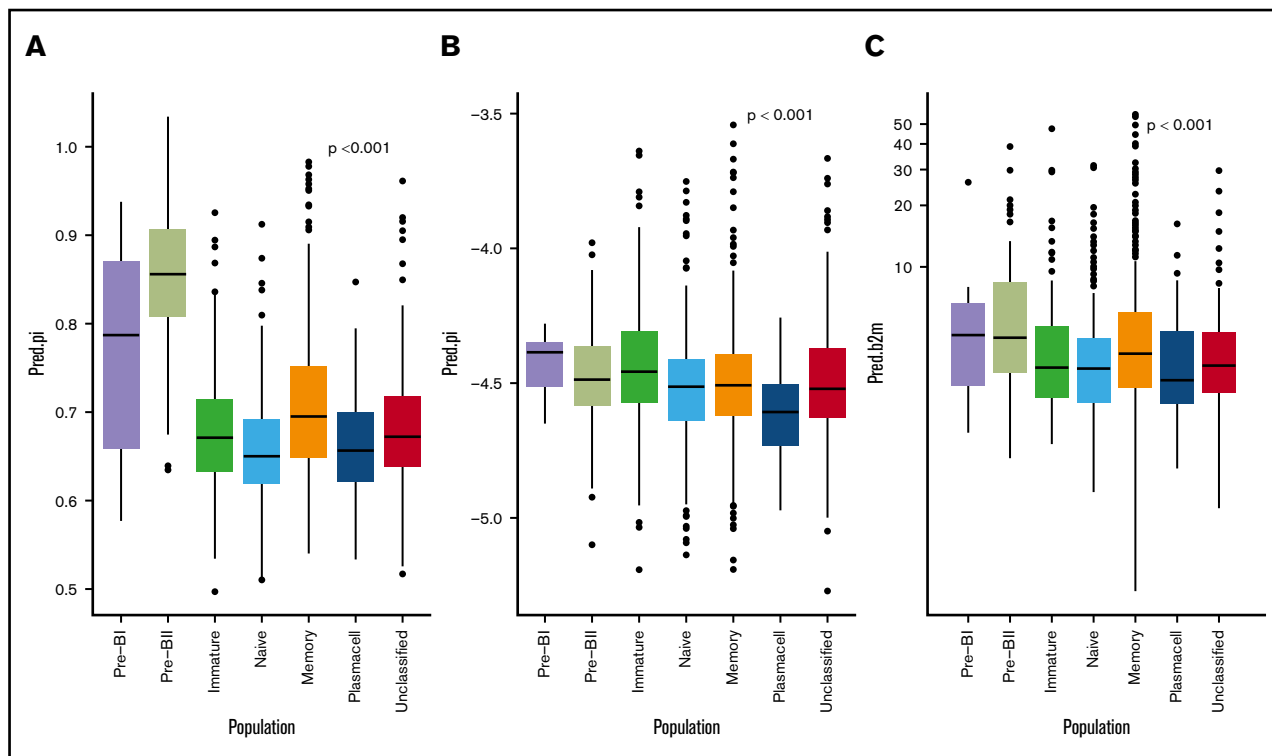
Figure 3. BAGS subtype boxplots with correlation to proliferation, melphalan resistance, and β-2 microglobulin. The individual adjusted PI risk profiling (A), melphalan drug resistance probability (index) (B), and β-2 microglobulin plasma level (C), respectively, per BAGS subtype cases from analysis of the meta–data set. The BAGS subtypes are color coded as in Figure 1.

5 of 6 PC leukemia cases were M subtypes, indicating a subtype evolution or selection for advanced disease. In contrast, MGUS cases had a significantly high frequency (>50%) of N subtypes, which was different from smoldering myeloma and newly diagnosed and relapsed MM. The distribution of M component isotypes showed no significant differences across BAGS subtypes, except for a tendency for light chain disease to be overrepresented in the postgerminal subtypes as shown in supplemental Table 7B. Frequencies of BAGS subtypes in relapsed MM patients from the APEX data set (supplemental Table 7C) were similar to the frequencies in first-line patients shown in Table 1. Finally, we observed that 9 out of 12 human myeloma cancer cell lines were classified as PC subtypes (supplemental Table 8).

Characterization of BAGS subtypes

Differential expression analysis of BAGS subtypes with poor prognosis (Pre-BII or memory vs rest) identified hundreds of genes with a highly significant differential expression as given in supplemental Table 9A-B for the Pre-BII and memory subtypes, respectively. GO enrichment of significant genes showed that the Pre-BII subtype myelomas are enriched for the categories mitotic cell cycle, nuclear division, and DNA-dependent DNA replication (supplemental Table 10A), and memory subtype myelomas are enriched for the categories cell-cell signaling, synaptic transmission, and multicellular organismal process (supplemental Table 10B). For more details, see supplemental Text 1.

Finally, in order to detect whether the Pre-BII and memory subtypes showed alternative splicing patterns associated with

oncogenesis, we investigated alternative exon usage in the IFM-DFCI data set. Results suggested Pre-BII-specific alternative exon usage for 16 genes (supplemental Table 1A), which were especially associated with biological processes involved in cell cycle regulation (supplemental Table 3A). In memory subtype cases, we only identified 2 candidate genes with potential alternative exon usage (supplemental Table 1B) associated with basic cell functions including regulation of programmed cell death, metabolism, and signaling transduction (supplemental Table 3B). Comparison with alternative exon usage patterns detected in nonmalignant samples (supplemental Table 11) indicated that the majority of events were specific to malignant samples, suggesting association to oncogenesis.

Discussion

We have phenotyped distinct cellular subsets of B-cells in the normal BM to generate a BAGS classifier and have documented that the assigned subtypes have prognostic impact.

A probability estimate for each sample to be assigned to each of the 6 BAGS subtypes was provided. Samples with very low classification probabilities were labeled as unclassified. The frequency of unclassified samples in other gene expression–based COO classifications is ~15%.[17] A pragmatic probability cutoff of 0.40 was used, which is well above the random assignment probability of 1 out of 6, to ensure that 85% of the samples would be BAGS subtypes. The robustness of the BAGS association with outcome was successfully assessed for a wide series of probability cutoffs.

The present study was whenever possible conducted according to guidelines of –omics-directed medicine (eg, McShane et al,[73] REMARK,[74] and MIAME[48]). However, it is worth noting that the BAGS classifier used cohort-based normalization, which implies that it cannot practically be used in a clinical setup where patients show up 1 at a time. Remedies to this problem have been proposed elsewhere[75] and were not further pursued here.

The assignment of BAGS subtypes to MM may explain an interindividual disease heterogeneity, which could reflect the association between cellular differentiation and oncogenesis.[27,76-78] A standardized flow cytometry immunophenotyping of hematological malignancies illustrates the potential clinical application of surface expressed markers to identify diagnostic tumor clones.[79] Such a strategy has allowed new studies of normal PC heterogeneity by differentiation.[6,10,80]

MM is an example of a malignant disease that has been studied intensively with microarrays. Many peer-reviewed papers have documented new classification systems based on gene expression profiles to correlate with biology and prognosis.[1,8-12] The present work addresses a need to study a new diagnostic platform defined by the molecular classification of BAGS in MM, as for DLBCL.[43,81] In accordance with our studies in DLBCL, where we applied the whole lymphoid differentiation compartment from tonsils or normal lymph nodes, we prospectively analyzed the lymphoid subset–defined compartments from normal BM to generate 6 BAGS for MM assignment. The idea was that the COO concept would hold true also for MM and assign subtypes from the postgerminal differentiation pathway. To our surprise, a major fraction of patient tissues were assigned a Pre-BII, Im, or N subtype, disproving the subtyping to be true reminiscence of the origin from a germinal or postgerminal phenotype. Given the phenotypic variation among MGUS, smoldering myeloma, MM, MM relapse, extramedullary MM, PC leukemia, and human myeloma cancer cell lines, it is more likely that BAGS assignment does classify MM cases based on reversible phenotypic plasticity.[33]

The BAGS classification is correlated to the well-established TC classification; however, we found that the poor prognosis for Pre-BII and memory subtypes correlated with the myeloma cell PI and the β-2 microglobulin plasma, but not gene expression level. PI and β-2 microglobulin is historically the most important and persistent biomarker in different trials, independent of the evolving therapy. The mechanisms behind these prognostically useful markers are unknown but should now be studied to understand their pathogenetic impact.

Our detection of alternative exon usage suggested subtype specific patterns, supporting that the BAGS phenotyping is based on biological processes. Alternatively spliced candidate genes detected in the Pre-BII subtype revealed an overrepresentation of genes involved in cell cycle regulation and increased proliferation, such as GTSE1, PKMYT1, BIRC5, and AURKB, suggesting an association with altered cell cycle regulation and proliferation. However, detected alternative exon usage of candidate genes needs to be experimentally validated and confirmed.

High-dose melphalan forms the basis of MM treatment.[82] However, patients with refractory or relapsed diseases represent a large unmet need for drug-specific predictive tests and precise companion diagnostics.[58,65-68] This need can be exemplified by REGS and BAGS classification with predictive information to guide therapy. The current analyses indicate that such information is available at diagnosis (Figure 3B; supplemental Figure 5B) and could be used for identification of candidates for more precise strategies. Collectively, this result indicates BAGS subtypes experience different clinical tracks and drug resistant mechanisms, and maybe even different molecular pathogenesis. We believe our results support the future inclusion of gene expression profiling in randomized prospective clinical trials aimed at improving MM treatment.

BAGS classification divided de novo MM patients into so-far-unrecognized, differentiation-dependent prognostic groups. These prognostic analyses and observations support the idea that BAGS classification in MM may contribute with pathogenetic information, especially in attempts to understand the biology behind the classical and still meaningful biomarkers PI and β-2 microglobulin. Most importantly, the classification included pregerminal subtypes, pointing at a reversible phenotypic plasticity in myeloma PCs. Prospective future studies are needed to prove the concept using clinical end points, including prediction of therapeutic outcome.

Acknowledgments

Authorship

Contribution: M.B. and K.D. designed the study, collected data, and led the study; J.S.B., R.F.B., A.S., M.B., and K.D. wrote the manuscript; R.F.B. and M.B. performed statistical analysis; J.S.B., K.D., A.A.S., D.S.J., T.E.-G., and H.E.J. provided biological and clinical interpretation; M.P.-A., A.O., A.S., R.F.B., A.A.S., M.S., C.V., H.D., C.H.N., D.S.J., P.J., M.A.N., R.S., and R.J.S. contributed vital technology or analytical tools; M.K.S., N.M., F.D., B.W., C.P., M.K., D.J., G.J.M., U.B., H.G., A.B., M.v.D., and P.S. delivered clinical and expression data; all authors read and approved the final version of the manuscript before submission; and H.E.J. led the project before his death and therefore contributed in designing the study and drafting the manuscript.

Conflict-of-interest disclosure: The authors declare no competing financial interests.

Hans Erik Johnson died on 17 May 2018.

ORCID profile: B.W., 0000-0002-8615-6254.

Correspondence: Martin Bøgsted, Department of Clinical Medicine, Aalborg University, Sdr. Skovvej 15, DK-9000 Aalborg, Denmark; e-mail: martin.boegsted@rn.dk.

References

1. Campo E, Swerdlow SH, Harris NL, Pileri S, Stein H, Jaffe ES. The 2008 WHO classification of lymphoid neoplasms and beyond: evolving concepts and practical applications. *Blood*. 2011;117(19):5019-5032.

2. Swerdlow SH, Campo E, Pileri SA, et al. The 2016 revision of the World Health Organization classification of lymphoid neoplasms. *Blood*. 2016;127(20):2375-2390.

3. Rasmussen T, Honoré L, Johnsen HE. Identification and characterisation of malignant cells using RT-PCR on single flow-sorted cells. *Med Oncol*. 1998;15(2):96-102.

4. Rasmussen T, Haaber J, Dahl IM, et al. Identification of translocation products but not K-RAS mutations in memory B cells from patients with multiple myeloma. *Haematologica*. 2010;95(10):1730-1737.

5. Kim D, Park CY, Medeiros BC, Weissman IL. CD19-CD45 low/- CD38 high/CD138+ plasma cells enrich for human tumorigenic myeloma cells. *Leukemia*. 2012;26(12):2530-2537.

6. Cenci S, van Anken E, Sitia R. Proteostenosis and plasma cell pathophysiology. *Curr Opin Cell Biol*. 2011;23(2):216-222.

7. Boise LH, Kaufman JL, Bahlis NJ, Lonial S, Lee KP. The Tao of myeloma. *Blood*. 2014;124(12):1873-1879.

8. Hallek M, Bergsagel PL, Anderson KC. Multiple myeloma: increasing evidence for a multistep transformation process. *Blood*. 1998;91(1):3-21.

9. Bergsagel PL, Kuehl WM, Zhan F, Sawyer J, Barlogie B, Shaughnessy J Jr. Cyclin D dysregulation: an early and unifying pathogenic event in multiple myeloma. *Blood*. 2005;106(1):296-303.

10. Zhan F, Hardin J, Kordsmeier B, et al. Global gene expression profiling of multiple myeloma, monoclonal gammopathy of undetermined significance, and normal bone marrow plasma cells. *Blood*. 2002;99(5):1745-1757.

11. Bergsagel PL, Kuehl WM. Chromosome translocations in multiple myeloma. *Oncogene*. 2001;20(40):5611-5622.

12. Bergsagel PL, Chesi M, Nardini E, Brents LA, Kirby SL, Kuehl WM. Promiscuous translocations into immunoglobulin heavy chain switch regions in multiple myeloma. *Proc Natl Acad Sci USA*. 1996;93(24):13931-13936.

13. Chesi M, Nardini E, Brents LA, et al. Frequent translocation t(4;14)(p16.3;q32.3) in multiple myeloma is associated with increased expression and activating mutations of fibroblast growth factor receptor 3. *Nat Genet*. 1997;16(3):260-264.

14. Rasmussen T, Theilgaard-Mönch K, Hudlebusch HR, Lodahl M, Johnsen HE, Dahl IM. Occurrence of dysregulated oncogenes in primary plasma cells representing consecutive stages of myeloma pathogenesis: indications for different disease entities. *Br J Haematol*. 2003;123(2):253-262.

15. Davies FE, Dring AM, Li C, et al. Insights into the multistep transformation of MGUS to myeloma using microarray expression analysis. *Blood*. 2003;102(13):4504-4511.

16. Rasmussen T, Kuehl M, Lodahl M, Johnsen HE, Dahl IMS. Possible roles for activating RAS mutations in the MGUS to MM transition and in the intramedullary to extramedullary transition in some plasma cell tumors. *Blood*. 2005;105(1):317-323.

17. Chapman MA, Lawrence MS, Keats JJ, et al. Initial genome sequencing and analysis of multiple myeloma. *Nature*. 2011;471(7339):467-472.

18. Egan JB, Shi CX, Tembe W, et al. Whole-genome sequencing of multiple myeloma from diagnosis to plasma cell leukemia reveals genomic initiating events, evolution, and clonal tides. *Blood*. 2012;120(5):1060-1066.

19. Leich E, Weißbach S, Klein H-U, et al. Multiple myeloma is affected by multiple and heterogeneous somatic mutations in adhesion- and receptor tyrosine kinase signaling molecules. *Blood Cancer J*. 2013;3:e102.

20. Vicente-Dueñas C, Romero-Camarero I, González-Herrero I, et al. A novel molecular mechanism involved in multiple myeloma development revealed by targeting MafB to haematopoietic progenitors. *EMBO J*. 2012;31(18):3704-3717.

21. Rasmussen T, Lodahl M, Hancke S, Johnsen HE. In multiple myeloma clonotypic CD38- /CD19+ / CD27+ memory B cells recirculate through bone marrow, peripheral blood and lymph nodes. *Leuk Lymphoma*. 2004;45(7):1413-1417.

22. Matsui W, Wang Q, Barber JP, et al. Clonogenic multiple myeloma progenitors, stem cell properties, and drug resistance. *Cancer Res*. 2008;68(1):190-197.

23. Paíno T, Ocio EM, Paiva B, et al. CD20 positive cells are undetectable in the majority of multiple myeloma cell lines and are not associated with a cancer stem cell phenotype. *Haematologica*. 2012;97(7):1110-1114.

24. Yaccoby S, Epstein J. The proliferative potential of myeloma plasma cells manifest in the SCID-hu host. *Blood*. 1999;94(10):3576-3582.

25. Guikema JEJ, Vellenga E, Bakkus MHC, Bos NA. Myeloma clonotypic B cells are hampered in their ability to undergo B-cell differentiation in vitro. *Br J Haematol*. 2002;119(1):54-61.

26. Rasmussen T, Jensen L, Johnsen HE. The clonal hierarchy in multiple myeloma. *Acta Oncol*. 2000;39(7):765-770.

27. Pfeifer S, Perez-Andres M, Ludwig H, Sahota SS, Zojer N. Evaluating the clonal hierarchy in light-chain multiple myeloma: implications against the myeloma stem cell hypothesis. *Leukemia*. 2011;25(7):1213-1216.

28. Van Valckenborgh E, Matsui W, Agarwal P, et al. Tumor-initiating capacity of CD138- and CD138+ tumor cells in the 5T33 multiple myeloma model. *Leukemia*. 2012;26(6):1436-1439.

29. Johnsen HE, Bøgsted M, Schmitz A, et al. The myeloma stem cell concept, revisited: from phenomenology to operational terms. *Haematologica*. 2016;101(12):1451-1459.

30. Hajek R, Okubote SA, Svachova H. Myeloma stem cell concepts, heterogeneity and plasticity of multiple myeloma. *Br J Haematol*. 2013;163(5):551-564.

31. Visvader JE. Cells of origin in cancer. *Nature*. 2011;469(7330):314-322.

32. Hanahan D, Weinberg RA. Hallmarks of cancer: the next generation. *Cell*. 2011;144(5):646-674.

33. Yaccoby S. The phenotypic plasticity of myeloma plasma cells as expressed by dedifferentiation into an immature, resilient, and apoptosis-resistant phenotype. *Clin Cancer Res*. 2005;11(21):7599-7606.

34. Bam R, Khan S, Ling W, et al. Primary myeloma interaction and growth in coculture with healthy donor hematopoietic bone marrow. *BMC Cancer*. 2015;15:864.

35. Zhan F, Huang Y, Colla S, et al. The molecular classification of multiple myeloma. *Blood*. 2006;108(6):2020-2028.

36. Mulligan G, Mitsiades C, Bryant B, et al. Gene expression profiling and correlation with outcome in clinical trials of the proteasome inhibitor bortezomib. *Blood*. 2007;109(8):3177-3188.

37. Avet-Loiseau H, Li C, Magrangeas F, et al. Prognostic significance of copy-number alterations in multiple myeloma. *J Clin Oncol*. 2009;27(27): 4585-4590.

38. Samur MK, Shah PK, Wang X, et al. The shaping and functional consequences of the dosage effect landscape in multiple myeloma. *BMC Genomics*. 2013;14:672.

39. Johnsen HE, Bergkvist KS, Schmitz A, et al; Myeloma Stem Cell Network (MSCNET). Cell of origin associated classification of B-cell malignancies by gene signatures of the normal B-cell hierarchy. *Leuk Lymphoma*. 2014;55(6):1251-1260.

40. Kjeldsen MK, Perez-Andres M, Schmitz A, et al. Multiparametric flow cytometry for identification and fluorescence activated cell sorting of five distinct B-cell subpopulations in normal tonsil tissue. *Am J Clin Pathol*. 2011;136(6):960-969.

41. Bergkvist KS, Nyegaard M, Bøgsted M, et al. Validation and implementation of a method for microarray gene expression profiling of minor B-cell subpopulations in man. *BMC Immunol*. 2014;15:3.

42. Rasmussen SM, Bilgrau AE, Schmitz A, et al. Stable phenotype of B-cell subsets following cryopreservation and thawing of normal human lymphocytes stored in a tissue biobank. *Cytometry B Clin Cytom*. 2015;88(1):40-49.

43. Dybkær K, Bøgsted M, Falgreen S, et al. Diffuse large B-cell lymphoma classification system that associates normal B-cell subset phenotypes with prognosis. *J Clin Oncol*. 2015;33(12):1379-1388.

44. Bergkvist KS, Nørgaard MA, Bøgsted M, et al. Characterization of memory B cells from thymus and its impact for DLBCL classification. *Exp Hematol*. 2016;44(10):982-990.

45. Michaelsen TY, Richter J, Brøndum RF, et al. A B-cell-associated gene signature classification of diffuse large B-cell lymphoma by NanoString technology. *Blood Adv*. 2018;2(13):1542-1546.

46. Nørgaard CH, Jakobsen LH, Gentles AJ, et al. Subtype assignment of CLL based on B-cell subset associated gene signatures from normal bone marrow - a proof of concept study. *PLoS One*. 2018;13(3):e0193249.

47. Petri A, Dybkær K, Bøgsted M, et al. Long noncoding RNA expression during human B-cell development. *PLoS One*. 2015;10(9):e0138236.

48. Brazma A, Hingamp P, Quackenbush J, et al. Minimum information about a microarray experiment (MIAME)-toward standards for microarray data. *Nat Genet*. 2001;29(4):365-371.

49. Barlogie B, Mitchell A, van Rhee F, Epstein J, Morgan GJ, Crowley J. Curing myeloma at last: defining criteria and providing the evidence. *Blood*. 2014; 124(20):3043-3051.

50. Broyl A, Hose D, Lokhorst H, et al. Gene expression profiling for molecular classification of multiple myeloma in newly diagnosed patients. *Blood*. 2010; 116(14):2543-2553.

51. Morgan GJ, Davies FE, Gregory WM, et al; National Cancer Research Institute Haematological Oncology Clinical Studies Group. Cyclophosphamide, thalidomide, and dexamethasone as induction therapy for newly diagnosed multiple myeloma patients destined for autologous stem-cell transplantation: MRC Myeloma IX randomized trial results. *Haematologica*. 2012;97(3):442-450.

52. Richardson PG, Sonneveld P, Schuster MW, et al; Assessment of Proteasome Inhibition for Extending Remissions (APEX) Investigators. Bortezomib or high-dose dexamethasone for relapsed multiple myeloma. *N Engl J Med*. 2005;352(24):2487-2498.

53. Chauhan D, Tian Z, Nicholson B, et al. A small molecule inhibitor of ubiquitin-specific protease-7 induces apoptosis in multiple myeloma cells and overcomes bortezomib resistance. *Cancer Cell*. 2012;22(3):345-358.

54. López-Corral L, Corchete LA, Sarasquete ME, et al. Transcriptome analysis reveals molecular profiles associated with evolving steps of monoclonal gammopathies. *Haematologica*. 2014;99(8):1365-1372.

55. Mattioli M, Agnelli L, Fabris S, et al. Gene expression profiling of plasma cell dyscrasias reveals molecular patterns associated with distinct IGH translocations in multiple myeloma. *Oncogene*. 2005;24(15):2461-2473.

56. Chng WJ, Kumar S, Vanwier S, et al. Molecular dissection of hyperdiploid multiple myeloma by gene expression profiling. *Cancer Res*. 2007;67(7): 2982-2989.

57. Tiedemann RE, Zhu YX, Schmidt J, et al. Kinome-wide RNAi studies in human multiple myeloma identify vulnerable kinase targets, including a lymphoid-restricted kinase, GRK6. *Blood*. 2010;115(8):1594-1604.

58. Falgreen S, Dybkær K, Young KH, et al. Predicting response to multidrug regimens in cancer patients using cell line experiments and regularised regression models. *BMC Cancer*. 2015;15:235.

59. Gentleman RC, Carey VJ, Bates DM, et al. Bioconductor: open software development for computational biology and bioinformatics. *Genome Biol*. 2004; 5(10):R80.

60. R Core Team. R: A Language and Environment for Statistical Computing. Vienna, Austria, Austria: R Foundation for Statistical Computing; 2017.

61. Xie Y. knitr: A General-Purpose Package for Dynamic Report Generation in R. Available at: https://cran.r-project.org/web/packages/knitr/index.html. Accessed 17 August 2018.

62. Irizarry RA, Hobbs B, Collin F, et al. Exploration, normalization, and summaries of high density oligonucleotide array probe level data. *Biostatistics*. 2003; 4(2):249-264.

63. Gautier L, Cope L, Bolstad BM, Irizarry RA. affy–analysis of Affymetrix GeneChip data at the probe level. *Bioinformatics*. 2004;20(3):307-315.

64. Friedman J, Hastie T, Tibshirani R. Regularization paths for generalized linear models via coordinate descent. *J Stat Softw*. 2010;33(1):1-22.

65. Boegsted M, Holst JM, Fogd K, et al. Generation of a predictive melphalan resistance index by drug screen of B-cell cancer cell lines. *PLoS One*. 2011; 6(4):e19322.

66. Bøgsted M, Bilgrau AE, Wardell CP, et al. Proof of the concept to use a malignant B cell line drug screen strategy for identification and weight of melphalan resistance genes in multiple myeloma. *PLoS One*. 2013;8(12):e83252.

67. Laursen MB, Falgreen S, Bødker JS, et al; Myeloma Stem Cell Network. Human B-cell cancer cell lines as a preclinical model for studies of drug effect in diffuse large B-cell lymphoma and multiple myeloma. *Exp Hematol*. 2014;42(11):927-938.

68. Falgreen S, Laursen MB, Bødker JS, et al. Exposure time independent summary statistics for assessment of drug dependent cell line growth inhibition. *BMC Bioinformatics*. 2014;15:168.

69. Therneau TM. A Package for Survival Analysis in S. Available at: https://cran.r-project.org/web/packages/survival/index.html. Accessed 17 August 2018.

70. Cline MS, Blume J, Cawley S, et al. ANOSVA: a statistical method for detecting splice variation from expression data. *Bioinformatics*. 2005;21(suppl 1): i107-i115.

71. Carlson M. GO.db: A set of annotation maps describing the entire Gene Ontology. Available at: https://bioconductor.org/packages/release/data/annotation/html/GO.db.html. Accessed 17 August 2018.

72. Holm S. A simple sequentially rejective multiple test procedure. *Scand J Stat*. 1979;6(2):65-70.

73. McShane LM, Cavenagh MM, Lively TG, et al. Criteria for the use of omics-based predictors in clinical trials: explanation and elaboration. *BMC Med*. 2013;11:220.

74. McShane LM, Altman DG, Sauerbrei W, Taube SE, Gion M, Clark GM; Statistics Subcommittee of the NCI-EORTC Working Group on Cancer Diagnostics. Reporting recommendations for tumor marker prognostic studies. *J Clin Oncol*. 2005;23(36):9067-9072.

75. Falgreen S, Ellern Bilgrau A, Brøndum RF, et al. hemaClass.org: online one-by-one microarray normalization and classification of hematological cancers for precision medicine. *PLoS One*. 2016;11(10):e0163711.

76. Greaves M, Maley CC. Clonal evolution in cancer. *Nature*. 2012;481(7381):306-313.

77. Corre J, Munshi N, Avet-Loiseau H. Genetics of multiple myeloma: another heterogeneity level? *Blood*. 2015;125(12):1870-1876.

78. Kuehl WM, Bergsagel PL. Multiple myeloma: evolving genetic events and host interactions. *Nat Rev Cancer*. 2002;2(3):175-187.

79. van Dongen JJM, Lhermitte L, Böttcher S, et al; EuroFlow Consortium (EU-FP6, LSHB-CT-2006-018708). EuroFlow antibody panels for standardized n-dimensional flow cytometric immunophenotyping of normal, reactive and malignant leukocytes. *Leukemia*. 2012;26(9):1908-1975.

80. Paiva B, Perez-Andres M, Gutierrez ML, et al. CD56+ clonal plasma cells in multiple myeloma are associated with unique disease characteristics and have a counterpart of CD56+ normal plasma cells with increased maturity [abstract]. *Blood*. 2013;122(21). Abstract 751.

81. Alizadeh AA, Eisen MB, Davis RE, et al. Distinct types of diffuse large B-cell lymphoma identified by gene expression profiling. *Nature*. 2000;403(6769): 503-511.

82. Engelhardt M, Terpos E, Kleber M, et al; European Myeloma Network. European Myeloma Network recommendations on the evaluation and treatment of newly diagnosed patients with multiple myeloma. *Haematologica*. 2014;99(2):232-242.